

Form-Stable Erythritol/HDPE Composite Phase Change Material with Flexibility, Tailorability, and High Transition Enthalpy

Siyu Chai,^{||} Keyan Sun,^{||} Donghui Zhao, Yan Kou, and Quan Shi*Cite This: <https://dx.doi.org/10.1021/acsapm.0c00584>

Read Online

ACCESS |



Metrics & More



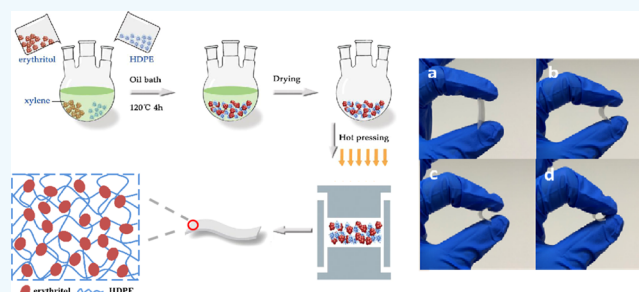
Article Recommendations



Supporting Information

ABSTRACT: Erythritol has attracted much attention recently in the field of phase change materials (PCMs) for thermal management because of its superior phase-transition properties. However, the liquid-phase leakage and solid-phase rigidity commonly existing in organic PCMs greatly limit its practical application. Herein, we have constructed a form-stable erythritol/high-density polyethylene (HDPE) composite PCM for the first time, in which erythritol serves as a PCM unit and HDPE as a supporting material. The most impressive aspect of this composite PCM is that the supporting material HDPE can also contribute extra transition enthalpy because of its overlapped melting temperature region with that of erythritol, and consequently, the constructed composite PCM exhibits a superior high melting enthalpy of 308.52 J/g. The erythritol/HDPE composite PCM reported in this work may provide a strategy of synthesizing from-stable PCMs with large thermal energy storage density. Moreover, we have further fabricated bulk erythritol/HDPE into a lamellar composite PCM with advanced flexibility and tailorability using a hot-pressing method. This lamellar shape-stable composite PCM is very promising to be utilized in the field of thermal management with a complicated application scenario or special configuration requirements.

KEYWORDS: phase change material, thermal management, erythritol, high-density polyethylene, form-stable, flexibility, tailorability



1. INTRODUCTION

At present, with the continuous development of human society, the consumption of nonrenewable energy sources such as fossil energy is huge, which imposes a serious burden on the global climate and environment. Because the supply and demand of energy sources often have mismatches in time and space, it is extremely important to have an advanced management technique for improving the energy utilization process with a more efficient, safe, and clean way. Phase change materials (PCMs) have attracted much attention in thermal management field in recent years because of their superior phase-transition properties of absorbing and releasing significant amounts of latent heats at almost constant temperatures, which can be utilized as thermal energy storage or temperature control units used for thermal management fields, such as solar energy thermal utilization, electronics or battery thermal management, and energy-saving buildings.^{1–4}

The main concern currently involved in PCM research field is to design and construct new materials with improved phase-transition properties for the purpose of increasing thermal management efficiency in the applications mentioned above and also with functional performance other than thermal properties to further expand the application field of PCMs. Sugar alcohols have been extensively studied recently in the PCM research field because of their attractive phase-transition

properties, low cost, nontoxicity, noncorrosivity, and non-flammability.^{5–7} Most importantly, theoretical studies have revealed that non-natural sugar alcohols could possess the largest transition enthalpy in the present known organic PCMs.^{8,9} Among various sugar alcohols, erythritol has been particularly concerned because of its relatively high phase-transition enthalpy (ΔH_M), which can be utilized as a promising medium-temperature PCM for thermal energy storage applications.^{10,11} However, the liquid-phase leakage and solid-phase rigidity commonly existing in organic PCMs greatly limit the practical application of erythritol.

In order to solve this problem, erythritol has usually been constructed into form-stable composites by loading it into supporting materials, and consequently, a large number of research works on erythritol-based composite PCMs have been extensively reported. For instance, Yuan et al. prepared an erythritol/EG (expanded graphite) composite PCM using an “impregnation, compression, and sintering” three-step method,

Received: May 31, 2020

Accepted: September 8, 2020

Published: September 8, 2020

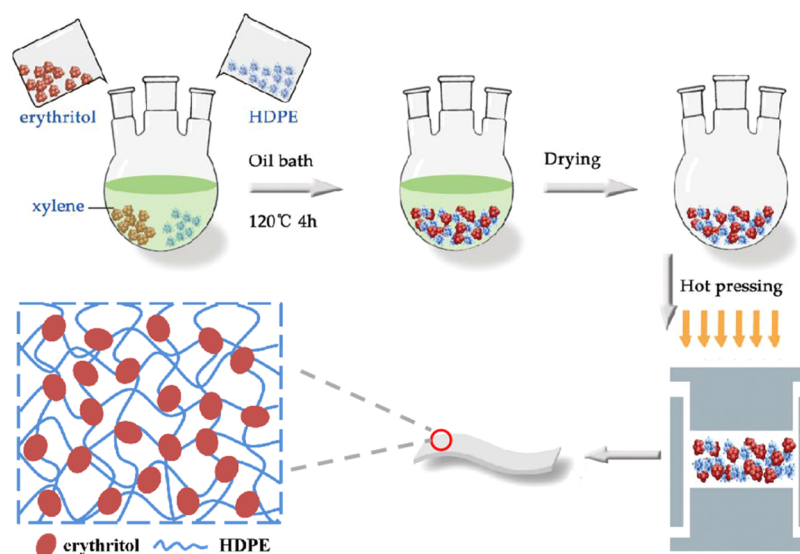


Figure 1. Process of preparing erythritol/HDPE composites.

and the composite phase-transition enthalpy was evaluated to be 212.50 J/g.⁵ Puupponen and Seppälä reported a form-stable erythritol composite using a cross-linked sodium polyacrylate as a supporting material, and a phase-transition enthalpy of 251.97 J/g could be realized for this composite.¹² Xiangfa et al. synthesized a form-stable silica aerogel/erythritol composite by means of a melting infiltration method, and the results indicated that the phase-transition enthalpy could reach as large as 289.92 J/g.¹³ Chen et al. performed a preparation and thermal energy storage property study on an erythritol/polyaniline form-stable PCM, in which the erythritol loading amounts in the composite could reach 75% and the melting enthalpy was about 260 J/g.¹⁴ Jiang et al. conducted further research by Chen et al. and added silver nanowires to the erythritol/polyaniline composite to improve the thermal conductivity, but the loading of erythritol was correspondingly lower, and the enthalpy value dropped to 220 J/g.¹⁵ Although these reported form-stable composites can effectively prevent the leakage of liquid-phase erythritol, and the latter composite material has higher phase-transition enthalpy, they all have a common problem that the addition of the supporting material without melting enthalpy contribution would greatly reduce the thermal energy storage density of erythritol and did not have application characteristics such as flexibility and plasticity. High-density polyethylene (HDPE) has been recently proposed as a supporting material for the preparation of myristic acid,¹⁶ paraffin waxes,^{3,17} and palmitic acid⁹ form-stable composite PCMs because of its low cost and high corrosion resistance to acids, alkalis, organic solvents, and various salts. It should be noticed that the melting temperature of HDPE is approximately 125 °C, which is very close to the erythritol melting transition temperature region. Although HDPE can melt above the melting temperature, the liquid phase of HDPE has no fluidity because of its high viscosity.^{17,18} Therefore, it can be predicted that liquid HDPE as a supporting material could still prevent the leakage of liquid erythritol. Moreover, HDPE can also exhibit a general plasticity as a polymer compound near the melting temperature region, and this plasticity may lead to a possibility of processing HDPE-based PCMs with a specific shape or configuration.

In the present work, we have employed HDPE as a supporting material for the first time to construct a form-stable erythritol/HDPE composite PCM with superior high melting enthalpy. HDPE can not only effectively prevent liquid erythritol from leaking even at its melting temperature region but also contribute extra phase-transition enthalpy to the composite PCM. The bulk erythritol/HDPE composite has been further processed into a flexible lamellar composite PCM. The sample morphology, composition, thermal performance, flexibility, and tailorability have been extensively investigated using various techniques. This work may provide a strategy for design and construction of a flexible form-stable composite PCM with high thermal energy storage density.

2. EXPERIMENTAL SECTION

2.1. Materials. Erythritol ($C_4H_{10}O_4$, $\geq 99\%$) was purchased from Dalian Meilun Biological Technology Co., Ltd. HDPE with an melt mass-flow rate of 0.25 g/10 min (190 °C/2.16 kg) and a density of 0.95 g/cm³ was provided by Alfa Aesar. Xylene (C_8H_{10} , $\geq 99\%$) was provided by Tianjin Damao Chemical Reagent Factory. All these starting materials were used without any further treatment.

2.2. Preparation of Erythritol/HDPE Composite. An erythritol/HDPE composite was synthesized using a solvent-assisted melting infiltration method. In general, erythritol and HDPE with various weight ratios ($w_{\text{Ery}}/w_{\text{PE}} = 60/40, 70/30, \text{ and } 80/20$) were added into a three-necked flask with xylene solvent (the ratio of HDPE to xylene solvent was 1 g/10 mL). The mixture was heated to 120 °C in an oil bath with continuous stirring for about 3 h to make erythritol fully infiltrate into HDPE. After that, the mixture was poured into a Petri dish and dried in an oven at 100 °C for about 12 h to evaporate out the xylene solvent. The form-stable erythritol/HDPE composite PCM was consequently obtained as shown in Figure 1 and named in Table 1 according to the starting material amounts used in

Table 1. Sample Name and Composition of Erythritol/HDPE Composites

| sample | erythritol (wt %) | HDPE (wt %) |
|-------------------|-------------------|-------------|
| HDPE | 0 | 100 |
| erythritol/HDPE40 | 60 | 40 |
| erythritol/HDPE30 | 70 | 30 |
| erythritol/HDPE20 | 80 | 20 |
| erythritol | 100 | 0 |

the synthesis. The bulk erythritol/HDPE20 sample was further ground into powder, loaded into a hot-pressing equipment for pressing at 150 °C for 10 min, and then cooled naturally to room temperature. Finally, a lamellar erythritol/HDPE composite with a thickness about 0.5 mm was obtained.

2.3. Characterization. The sample surface morphology and microstructure were detected using a scanning electron microscope (JSM-7800F, Japan) with a 3 kV acceleration voltage. Phase compositions were analyzed by a powder X-ray diffractometer (X'pert Pro-1, PANalytical) with a Cu K α radiation ($\lambda = 0.1514$ nm). Chemical structure analysis was performed on a Fourier transform infrared (FTIR) spectrometer through KBr tableting (Nicolet iS50, Thermo Fisher Scientific, spectral range: 400–4000 cm⁻¹). A thermogravimetric analyzer (SETSYS 16/18, SETARAM, France) was employed to analyze the thermal stability of the sample from room temperature to 600 °C with a heat rate of 10 °C/min under a nitrogen atmosphere. The phase-transition property was investigated using a differential scanning calorimeter (204HP, Netzsch, German). The melting temperature is obtained by extrapolating the onset temperature of the transition region of the differential scanning calorimetry (DSC) curve, and the phase change enthalpy is obtained by integrating the temperature and heat flow of the DSC curve. The measurement uncertainty of temperature is in the range of ± 0.1 °C and the enthalpy uncertainty is in the range of $\pm 5\%$. The DSC measurement was carried out for two cycles in the temperature range of -80 to 200 °C with a heat rate of 10 °C/min and a nitrogen flow rate of 20 mL/min. The DSC data collected in the second run were used to analyze the sample phase-transition property.

3. RESULTS AND DISCUSSION

3.1. Shape Stability, Tailorability, and Flexibility. The shape stability of the erythritol/HDPE composites was evaluated by heating them at 125 °C for 4 h and then checking their shape change and liquid leakage behavior. It should point out that the melting temperature of the erythritol sample used in this work is about 119 °C, and therefore, at 125 °C heating temperature, erythritol should be totally in liquid phase. In order to clearly observe the sample changes, the erythritol/HDPE composites as well as a pure erythritol sample were placed on a filter paper in the test, and the photos of these samples taken before and after heating are presented in Figure 2. It can be seen from the figure that the pure

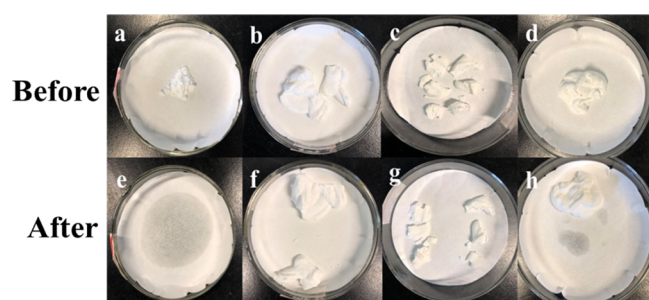


Figure 2. Sample photos of erythritol (a,e), erythritol/HDPE40 (b,f), erythritol/HDPE30 (c,g), and erythritol/HDPE20 (d,h) taken before and after heating at 125 °C.

erythritol is melted into liquid and completely absorbed by the filter paper after the heating process. As for the composites, all these samples may become slightly soft but still maintain their original shapes after the heating process, indicating that the HDPE supporting material can effectively maintain the shape stability of the composites. Also, there is no leakage traces detected in the filter paper for erythritol/HDPE40 and erythritol/HDPE30, and only a very small amount of liquid

trace is found for erythritol/HDPE20, suggesting that the HDPE supporting material can encapsulate the erythritol PCM well and effectively prevent the leakage of the liquid phase. Because the liquid-phase leakage in the erythritol/HDPE20 sample is so small, the maximum erythritol weight percent loaded in our erythritol/HDPE composite can be achieved to 80% approximately.

The erythritol/HDPE20 sample was further fabricated into a lamellar composite PCM using a hot-pressing method. This lamellar composite can be easily tailored into various shapes, such as square, circular, moon, heart, and star. It can be noticed that there are some little white dots appearing on the lamellar surface, which is likely due to a small amount of erythritol absorbed on the composite surface and may be crystallized separately because of its significant undercooling behavior. These interesting shaped composites are demonstrated in Figure 3a, indicating that the lamellar erythritol/HDPE



Figure 3. (a) Lamellar erythritol/HDPE20 with various shapes and (b) flexibility demonstration of square-shaped lamellar erythritol/HDPE20 with different bending angles.

composite PCM prepared in this work can exhibit an outstanding tailorability. Besides, the lamellar composite also shows an excellent flexibility. As can be seen in Figure 3b, the square-shaped composite was bent with different angles without any breaking, and it still can possess good flexibility even with a 180° bending angle. This advanced tailorability and flexibility possessed in our lamellar composite should likely be resulted from the intrinsic toughness and mechanical property of the HDPE supporting material. It can be predicted that the erythritol/HDPE composite PCM constructed in our work may have a promising application in the thermal management field with complicated scenarios or special configuration requirements.

3.2. SEM, FTIR, and XRD Characterization. The microscopic structure of the erythritol/HDPE composite as well as the pure erythritol and HDPE sample was inspected using a scanning electron microscopy (SEM), and the corresponding SEM images are presented in Figure 4. It can be seen that the HDPE surface is uniform and smooth, while the erythritol involves irregular-shaped particles stacked together with a smooth surface and a size of about several microns. As for the composite, it can be observed that erythritol still maintains its original irregular particle state, while HDPE shows an interesting “adhesive” structure adhering to the surface of each erythritol particle and glueing these particles together. This interesting “adhesive” structure

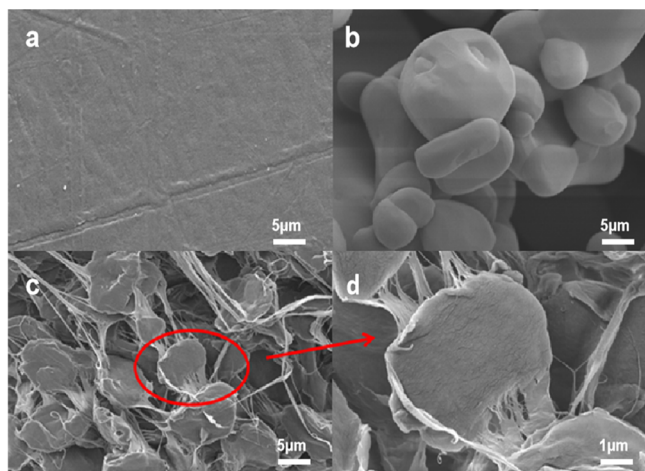


Figure 4. SEM images of HDPE (a), erythritol (b), and erythritol/HDPE20 (c,d).

formed in HDPE is likely to account for the superior shape stability, tailorability, and flexibility exhibited in our erythritol/HDPE composite.

The chemical structure of the erythritol/HDPE20, pure erythritol, and HDPE samples was also investigated by means of FTIR measurement, and the obtained FTIR spectrum for these samples is presented in Figure 5. In the FTIR spectrum of HDPE, the peaks at 717, 1470, 2850, and 2912 cm^{-1} should be assigned to out-of-plane bending vibration, in-plane bending vibration of C–H, and symmetric and asymmetric stretching vibration of C–H, respectively. In the FTIR spectrum of erythritol, the peak at 3259 cm^{-1} represents the stretching vibration of O–H, and the peaks at 2912 and 2970 cm^{-1} can be assigned to the symmetric and asymmetric stretching vibration of C–H, respectively. The peaks at 1416 and 1258 cm^{-1} should represent the in-plane bending vibration of C–H, and the peaks at 1055 and 1082 cm^{-1} stand for C–C skeleton stretching vibration. In addition, the typical adsorption peak of out-of-plane swing vibration of –OH is located at 969 cm^{-1} , and the peaks at 882 and 709 cm^{-1} represent the out-of-plane bending vibration of C–H. The out-of-plane bending vibration of 1000–650 cm^{-1} represents that there are four or more –CH₂ groups in the erythritol chain.^{19–22} As for the composite, the FTIR spectrum reveals that all the peaks mentioned above for HDPE and erythritol are included in this composite, and no other additional peaks can be detected. This suggests that there is no chemical bonding formed between HDPE and erythritol, and the

physical adhesive force between them should be responsible for the form-stability of the erythritol/HDPE composite. Furthermore, in the X-ray diffraction (XRD) spectrum of HDPE, erythritol, and erythritol/HDPE20, the pure HDPE crystal unit cell exhibits a monoclinic characteristic, and it can be seen that there are three main peaks located at 21.8°, 24.2°, and 36.5°, attributing to the crystal planes of (110), (200), and (020).^{23–25} As shown in the pattern of erythritol, the strong peaks located at 14.7°, 19.6°, 20.2°, 24.5°, and 29.6° are attributed to the characteristics of erythritol, which are in accordance with the previous reports.^{26–28} For the composite, the XRD pattern shows that no new characteristic peaks appeared, which further confirms that the composite is constructed only by a physical combination of erythritol and HDPE.^{29,30}

3.3. Thermal Stability and Phase-Transition Property.

The thermogravimetric measurement was performed to determine the thermal stability of the erythritol, HDPE, and erythritol/HDPE composites. The thermogravimetric analysis (TGA) and derivative thermogravimetric (DTG) curves are shown in Figure 6, and the corresponding decomposition

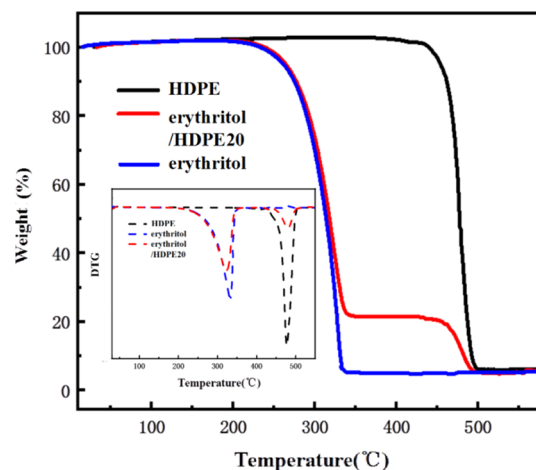


Figure 6. TGA and DTG curves of HDPE, erythritol, and erythritol/HDPE20.

parameters are summarized in Table 2. As the TGA and derivative thermogravimetric analysis curves show, both erythritol and HDPE show a similar one-step decomposition with onset temperatures of 301.09 and 465.38 °C, respectively, revealing that the HDPE supporting material is more thermally stable than erythritol. As for the composite, it is not surprising

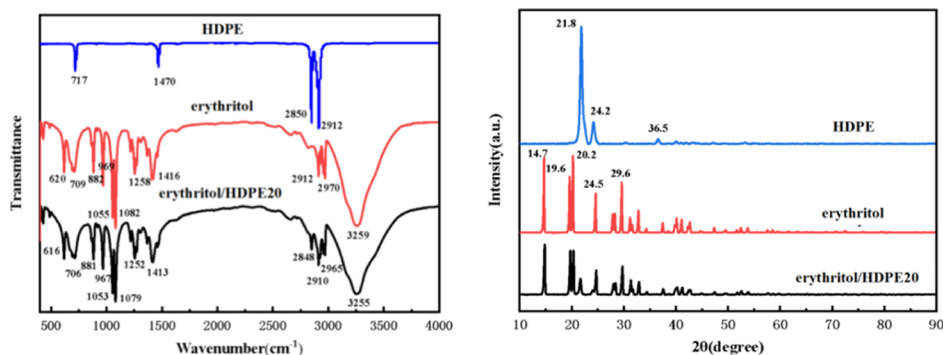


Figure 5. FTIR (left) and XRD (right) spectrum of HDPE, erythritol, and erythritol/HDPE20.

Table 2. Decomposition Parameters of Erythritol, HDPE, and Erythritol/HDPE20 from TGA Measurement

| sample | T_{onset1} (°C) | T_{peak1} (°C) | ΔW_1 (%) | T_{onset2} (°C) | T_{peak2} (°C) | ΔW_2 (%) |
|-------------------|--------------------------|-------------------------|------------------|--------------------------|-------------------------|------------------|
| erythritol | 301.04 | 333.83 | 98.86 | / | / | / |
| HDPE | / | / | / | 465.43 | 476.94 | 96.54 |
| erythritol/HDPE20 | 292.90 | 322.45 | 80.50 | 462.21 | 481.25 | 16.39 |

to find a two-step decomposition with onset temperatures of 292.90 and 462.21 °C, which are corresponding to the decomposition of erythritol and HDPE, respectively. These results suggest that the erythritol/HDPE composite is thermally stable in the temperature region below 292.90 °C. It should be pointed out that the composite decomposition temperature is slightly lower than that of pure erythritol and HDPE, which should stem from the physical interaction between erythritol and HDPE, likely promoting their decomposition at lower temperatures.^{31,32} Additionally, the weight loss in the composite is 81.15 and 18.85% in the first and second decomposition step, respectively, which is almost in agreement with the erythritol/HDPE mass ratio of the erythritol/HDPE20 sample used in the synthesis procedure.

The DSC technique was used to explore the phase-transition properties of the erythritol, HDPE, and erythritol/HDPE composites, and the corresponding results are shown in Figure 7 and listed Table 3. As can be seen in the melting process,

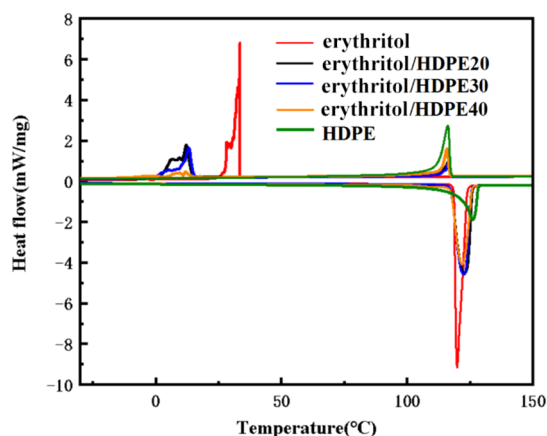


Figure 7. DSC curves of erythritol, HDPE, and erythritol/HDPE composites.

both erythritol and HDPE exhibit a phase transition with onset temperatures of 118.60 and 121.03 °C, respectively, and these temperature onsets are so close that the phase transition of these two compounds are overlapped in one temperature region. Consequently, it is not surprising to observe that the erythritol/HDPE composite behaves a single continuous transition in this overlapped temperature region. However, in the crystallizing process, the phase-transition regions of

erythritol and HDPE are separated obviously from each other because of the significant subcooling behavior generally existing in erythritol.^{6–8} The crystallization onset temperature of both pure HDPE and supporting HDPE in the composite is about 117 °C, suggesting that erythritol could hardly affect the HDPE crystallization behavior. As for the erythritol, the crystallization onset temperature is about 33 °C for the pure sample and about 14 °C for the sample in the composites, indicating that the physical interaction from the HDPE matrix may lower the erythritol crystallization temperature.^{32–34}

As for the transition enthalpy shown in Table 3, the melting enthalpy of erythritol/HDPE20 is slightly smaller than that of erythritol and much larger than that of HDPE and increases with the increase of erythritol contents in the composite. A maximum melting enthalpy can be achieved as high as 308.52 J/g in the erythritol/HDPE20. We have compared the melting enthalpy of our erythritol/HDPE20 composite with that of other related PCM composites in Table S1 (shown in the Supporting Information), and it can be seen that erythritol/HDPE20 possesses a comparably large melting enthalpy in these erythritol-based form-stable PCMs^{5,12–15,19,39} and exhibits the largest melting enthalpy reported in the literature for flexible PCMs^{35–38} as far as we know. In order to have accurate erythritol and HDPE contents in the composites, we have employed the melting enthalpy listed in Table 3 in the flowing equation^{40,41}

$$\Delta H_{M,A}x_A + \Delta H_{M,B}x_B = \Delta H_{M,FSPCM} \quad (1)$$

$$x_A + x_B = 100 \quad (2)$$

where x_A and x_B represent the weight percent of erythritol and HDPE in the composite, respectively. $\Delta H_{M,A}$, $\Delta H_{M,B}$, and $\Delta H_{M,FSPCM}$ are melting enthalpies listed in Table 3 for the erythritol, HDPE, and erythritol/HDPE composites, respectively. The calculation results for x_A and x_B are also presented in the last two columns of Table 3. It can be found that the erythritol weight percent calculated using these equations is slightly lower than that of the starting material ratios listed in Table 1, which is likely due to the erythritol loss in the composite synthesis process, such as sample transfer from the three-necked flask to the Petri dish or long-time evaporation of xylene in the oven at 100 °C. In the erythritol/HDPE20 composite, the weight percent for erythritol and HDPE is about 80 and 20%, and the melting enthalpy contribution calculated using their pure sample enthalpy from Table 3 is about 76.16 and 23.84%, respectively. Compared with other

Table 3. Phase-Transition Parameters of Erythritol, HDPE, and Erythritol/HDPE Composites from DSC Measurement

| samples | melting | | | crystallization | | | x_A (%) | x_B (%) |
|-------------------|------------|--------------------|----------------|------------------------|----------------|------------------------|-----------|-----------|
| | T_M (°C) | ΔH_M (J/g) | $T_{C,1}$ (°C) | $\Delta H_{C,1}$ (J/g) | $T_{C,2}$ (°C) | $\Delta H_{C,2}$ (J/g) | | |
| erythritol | 118.60 | 347.71 | 33.31 | 202.25 | / | / | 100 | 0 |
| erythritol/HDPE20 | 117.41 | 308.52 | 14.36 | 126.38 | 117.12 | 25.73 | 76.16 | 23.84 |
| erythritol/HDPE30 | 117.65 | 285.16 | 14.90 | 106.30 | 117.24 | 28.50 | 61.95 | 38.05 |
| erythritol/HDPE40 | 117.37 | 267.79 | 13.89 | 32.85 | 116.80 | 49.78 | 53.17 | 47.83 |
| HDPE | 121.03 | 183.31 | / | / | 117.29 | 179.44 | 0 | 100 |

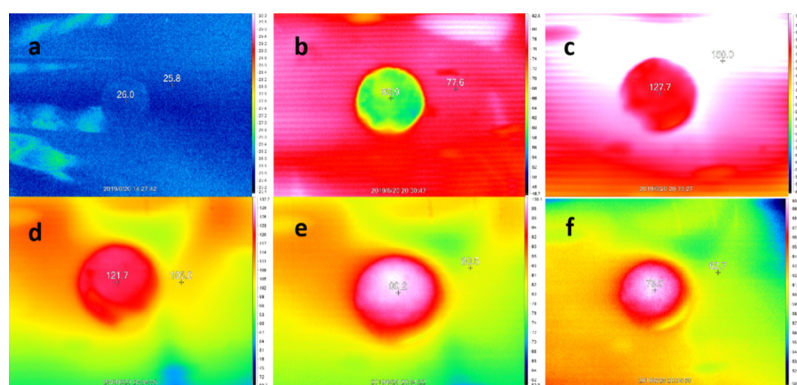


Figure 8. Thermographic images of erythritol/HDPE20 in (a–c) heating process and (d–f) cooling process.

supporting materials without the phase-transition function, HDPE can contribute 23.84% extra melting enthalpy to the erythritol-based form-stable PCMs, suggesting a promising strategy of constructing form-stable PCMs with high thermal energy storage density.

3.4. Thermal Management Performance. In order to evaluate the thermal management performance of the erythritol/HDPE composite, the circle-shaped lamellar sample shown in Figure 3a was placed on a heating sheet and continuously heated from room temperature to 150 °C, and the temperature change was recorded by an infrared imager (Fluke Ti400). Figure 8 shows the comparison of the temperature between the heating background and the composite PCM during the heating and cooling processes. As we can see from Figure 8a–c, in the heating process, the temperature of the composite PCM increases with the increase of heating time, while obviously lower than that of background, representing that the thermal energy is stored in the composite PCM. As the heating source is removed, the temperature of both the composite PCM and background naturally decreases; from Figure 8d–f, we can observe that the composite PCM temperature is relatively higher than that of the background, indicating that the composite PCM releases its latent heat during this cooling process. These results illuminate that this circle-shaped lamellar composite PCM can obviously manage the thermal energy as the background temperature changes using its phase-transition performance. Also, as demonstrated above, our lamellar composite PCM can be tailored into various shapes and exhibit an outstanding flexibility and superior high melting enthalpy, suggesting that this form-stable erythritol/HDPE developed in this work may have very promising applications for advanced thermal management techniques in the future.

4. CONCLUSIONS

In summary, we have reported a form-stable erythritol/HDPE composite PCM, for the first time, with advanced flexibility and tailorability and superior high transition enthalpy for thermal management applications in the present work. The erythritol/HDPE composite has been synthesized using a facile solvent-assisted melting infiltration method and then easily fabricated into a lamellar composite PCM by means of a hot-pressing process. Most impressively, the lamellar composite PCM has been tailored into various configurations, showing good flexibility in solid-phase state. The SEM, FTIR, and XRD investigations have revealed that the erythritol PCM is effectively adhered by the HDPE supporting material through

their physical interaction, preventing liquid-phase erythritol leakage from the composite to result in a form-stable PCM. Additionally, the melting transition enthalpy of the composite has been determined to be 308.52 J/g, in which not only erythritol but also the HDPE supporting material can contribute transition enthalpy to the composite. This superior high melting enthalpy is the largest as reported in the literature for flexible PCMs as far as we know. The lamellar composite PCM has also demonstrated an obvious thermal management performance in a specifically tailored configuration, exhibiting an attracting utilization in thermal management with a complicated application scenario or special configuration requirements. Based on these advanced performances, this erythritol/HDPE composite PCM constructed in our work may have promising applications for the development of next-generation thermal management technology.

■ ASSOCIATED CONTENT

Supporting Information

The Supporting Information is available free of charge at <https://pubs.acs.org/doi/10.1021/acsapm.0c00584>.

Comparison of phase change enthalpy of reported form-stable PCMs and SEM images of erythritol/HDPE30 and erythritol/HDPE40 (PDF)

■ AUTHOR INFORMATION

Corresponding Author

Quan Shi – Thermochemistry Laboratory, Chinese Academy of Sciences, Liaoning Province Key Laboratory of Thermochemistry for Energy and Materials, Dalian National Laboratory for Clean Energy, Dalian Institute of Chemical Physics, Dalian 116023, PR China; orcid.org/0000-0002-8792-0533; Email: shiquan@dicp.ac.cn

Authors

Siyu Chai – Thermochemistry Laboratory, Chinese Academy of Sciences, Liaoning Province Key Laboratory of Thermochemistry for Energy and Materials, Dalian National Laboratory for Clean Energy, Dalian Institute of Chemical Physics, Dalian 116023, PR China; University of Chinese Academy of Sciences, Beijing 100049, PR China

Keyan Sun – Thermochemistry Laboratory, Chinese Academy of Sciences, Liaoning Province Key Laboratory of Thermochemistry for Energy and Materials, Dalian National Laboratory for Clean Energy, Dalian Institute of Chemical Physics, Dalian 116023, PR China; University of Chinese Academy of Sciences, Beijing 100049, PR China

Donghui Zhao – School of Art and Design, Dalian Jiaotong University, Dalian 116028, PR China

Yan Kou – Thermochemistry Laboratory, Chinese Academy of Sciences, Liaoning Province Key Laboratory of Thermochemistry for Energy and Materials, Dalian National Laboratory for Clean Energy, Dalian Institute of Chemical Physics, Dalian 116023, PR China

Complete contact information is available at:
<https://pubs.acs.org/10.1021/acsapm.0c00584>

Author Contributions

[†]S.C. and K.S. contributed equally to this work.

Notes

The authors declare no competing financial interest.

ACKNOWLEDGMENTS

This work was financially supported by the National Natural Science Foundation of China under grant no. 21903082, the Liaoning Provincial Natural Science Foundation of China under grant no. 2019-MS-318, the Science and Technology Major Project of Liaoning Province (2019) under grant no. 2019JH1/10300002, the Scientific Instrument Developing Project of the Chinese Academy of Sciences under grant no. YJKYYQ20190046, and DICP under grant no. DICP I202036. Q.S. would like to thank the Dalian Outstanding Young Scientific Talent Program.

REFERENCES

- (1) Gunasekara, S. N.; Pan, R.; Chiu, J. N.; Martin, V. Polyols as phase change materials for surplus thermal energy storage. *Appl. Energy* **2016**, *162*, 1439–1452.
- (2) Zhang, Y.; Li, X.; Li, J.; Ma, C.; Guo, L.; Meng, X. Solar-driven phase change microencapsulation with efficient Ti_4O_7 nanoconverter for latent heat storage. *Nano Energy* **2018**, *53*, 579–586.
- (3) Cai, Y.; Wei, Q.; Huang, F.; Gao, W. Preparation and properties studies of halogen-free flame retardant form-stable phase change materials based on paraffin/high density polyethylene composites. *Appl. Energy* **2008**, *85*, 765–775.
- (4) Wang, L.; Meng, D. Fatty acid eutectic/polymethyl methacrylate composite as form-stable phase change material for thermal energy storage. *Appl. Energy* **2010**, *87*, 2660–2665.
- (5) Yuan, M.; Ren, Y.; Xu, C.; Ye, F.; Du, X. Characterization and stability study of a form-stable erythritol/expanded graphite composite phase change material for thermal energy storage. *Renew. Energy* **2019**, *136*, 211–222.
- (6) Solé, A.; Neumann, H.; Niedermaier, S.; Martorell, I.; Schossig, P.; Cabeza, L. F. Stability of sugar alcohols as PCM for thermal energy storage. *Sol. Energy Mater. Sol. Cells* **2014**, *126*, 125–134.
- (7) Dierce, G.; Gandarias, I.; Campos-Celador, Á.; García-Romero, A.; Griesser, U. J. Eutectic mixtures of sugar alcohols for thermal energy storage in the 50–90°C temperature range. *Sol. Energy Mater. Sol. Cells* **2015**, *134*, 215–226.
- (8) Jia, R.; Sun, K.; Li, R.; Zhang, Y.; Wang, W.; Yin, H.; Fang, D.; Shi, Q.; Tan, Z. Heat capacities of some sugar alcohols as phase change materials for thermal energy storage applications. *J. Chem. Therm.* **2017**, *115*, 233–248.
- (9) Inagaki, T.; Ishida, T. Computational Analysis of Sugar Alcohols as Phase-Change Material: Insight into the Molecular Mechanism of Thermal Energy Storage. *J. Phys. Chem. C* **2016**, *120*, 7903–7915.
- (10) Qi, G.; Yang, J.; Bao, R.; Xia, D.; Cao, M.; Yang, W.; Yang, M.; Wei, D. Hierarchical graphene foam-based phase change materials with enhanced thermal conductivity and shape stability for efficient solar-to-thermal energy conversion and storage. *Nano Res.* **2016**, *10*, 802–813.
- (11) Rao, Z.; Zhang, G.; Xu, T.; Hong, K. Experimental study on a novel form-stable phase change materials based on diatomite for solar energy storage. *Sol. Energy Mater. Sol. Cells* **2018**, *182*, 52–60.
- (12) Puupponen, S.; Seppälä, A. Cold-crystallization of polyelectrolyte absorbed polyol for long-term thermal energy storage. *Sol. Energy Mater. Sol. Cells* **2018**, *180*, 59–66.
- (13) Xiangfa, Z.; Hanning, X.; Jian, F.; Changrui, Z.; Yonggang, J. Preparation, properties and thermal control applications of silica aerogel infiltrated with solid–liquid phase change materials. *J. Exp. Nanosci.* **2012**, *7*, 17–26.
- (14) Chen, Y.-H.; Jiang, L.-M.; Fang, Y.; Shu, L.; Zhang, Y.-X.; Xie, T.; Li, K.-Y.; Tan, N.; Zhu, L.; Cao, Z.; Zeng, J.-L. Preparation and thermal energy storage properties of erythritol/polyaniline form-stable phase change material. *Sol. Energy Mater. Sol. Cells* **2019**, *200*, 109989.
- (15) Jiang, L.-M.; Chen, Y.-H.; Shu, L. Preparation and characterization of erythritol/polyaniline form-stable phase change materials containing silver nanowires. *Int. J. Energy Res.* **2019**, *43*, 8385–8397.
- (16) Tang, Y.; Su, D.; Huang, X.; Alva, G.; Liu, L.; Fang, G. Synthesis and thermal properties of the MA/HDPE composites with nano-additives as form-stable PCM with improved thermal conductivity. *Appl. Energy* **2016**, *180*, 116–129.
- (17) Mu, M.; Basheer, P. A. M.; Sha, W.; Bai, Y.; McNally, T. Shape stabilised phase change materials based on a high melt viscosity HDPE and paraffin waxes. *Appl. Energy* **2016**, *162*, 68–82.
- (18) Tang, Y.; Jia, Y.; Alva, G.; Huang, X.; Fang, G. Synthesis, characterization and properties of palmitic acid/high density polyethylene/graphene nanoplatelets composites as form-stable phase change materials. *Sol. Energy Mater. Sol. Cells* **2016**, *155*, 421–429.
- (19) An, J.; Liang, W.; Mu, P.; Wang, C.; Chen, T.; Zhu, Z.; Sun, H.; Li, A. Novel Sugar Alcohol/Carbonized Kapok Fiber Composites as Form-Stable Phase-Change Materials with Exceptionally High Latent Heat for Thermal Energy Storage. *ACS Omega* **2019**, *4*, 4848–4855.
- (20) Zhou, Y.; Wang, X.; Liu, X.; Sheng, D.; Ji, F.; Dong, L.; Xu, S.; Wu, H.; Yang, Y. Polyurethane-based solid-solid phase change materials with halloysite nanotubes-hybrid graphene aerogels for efficient light- and electro-thermal conversion and storage. *Carbon* **2019**, *142*, 558–566.
- (21) Shin, B.-S.; Seo, D.-K.; Kim, H.-B.; Jeun, J.-P.; Kang, P.-H. A study of the thermal and mechanical properties of electron beam irradiated HDPE/EPDM blends in the presence of triallyl cyanurate. *J. Ind. Eng. Chem.* **2012**, *18*, 526–531.
- (22) Zhang, P.; Xiao, X.; Ma, Z. W. A review of the composite phase change materials: Fabrication, characterization, mathematical modeling and application to performance enhancement. *Appl. Energy* **2016**, *165*, 472–510.
- (23) Jin, X.; Li, J.; Xue, P.; Jia, M. Preparation and characterization of PVC-based form-stable phase change materials. *Sol. Energy Mater. Sol. Cells* **2014**, *130*, 435–441.
- (24) Şentürk, S. B.; Kahraman, D.; Alkan, C.; Gökçe, İ. Biodegradable PEG/cellulose, PEG/agarose and PEG/chitosan blends as shape stabilized phase change materials for latent heat energy storage. *Carbohydr. Polym.* **2011**, *84*, 141–144.
- (25) Tang, B.; Wang, Y.; Qiu, M.; Zhang, S. A full-band sunlight-driven carbon nanotube/PEG/SiO₂ composites for solar energy storage. *Sol. Energy Mater. Sol. Cells* **2014**, *123*, 7–12.
- (26) Alkan, C.; Günther, E.; Hiebler, S.; Himpel, M. Complexing blends of polyacrylic acid-polyethylene glycol and poly(ethylene-co-acrylic acid)-polyethylene glycol as shape stabilized phase change materials. *Energy Convers. Manag.* **2012**, *64*, 364–370.
- (27) Paul, A.; Shi, L.; Bielawski, C. W. A eutectic mixture of galactitol and mannitol as a phase change material for latent heat storage. *Energy Convers. Manag.* **2015**, *103*, 139–146.
- (28) Yuan, P.; Zhang, P.; Liang, T.; Zhai, S.; Yang, D. Effects of functionalization on energy storage properties and thermal conductivity of graphene/n-octadecane composite phase change materials. *J. Mater. Sci.* **2018**, *54*, 1488–1501.
- (29) Shirkavand, M. J.; Azizi, H.; Ghasemi, I.; Karabi, M. Effect of Molecular Structure Parameters on Crystallinity and Environmental

Stress Cracking Resistance of High-Density Polyethylene/TiO₂ Nanocomposites. *Adv. Polym. Technol.* **2018**, *37*, 770–777.

(30) Lopes Jesus, A. J.; Nunes, S. C. C.; Ramos Silva, M.; Matos Beja, A.; Redinha, J. S. Erythritol: crystal growth from the melt. *Int. J. Pharm.* **2010**, *388*, 129–135.

(31) Tanimura, S.; Tahara, K.; Takeuchi, H. Spray-dried composite particles of erythritol and porous silica for orally disintegrating tablets prepared by direct tableting. *Powder Technol.* **2015**, *286*, 444–450.

(32) Zhang, X.; Huang, Z.; Ma, B.; Wen, R.; Min, X.; Huang, Y.; Yin, Z.; Liu, Y.; Fang, M.; Wu, X. Preparation and performance of novel form-stable composite phase change materials based on polyethylene glycol/White Carbon Black assisted by super-ultrasound-assisted. *Thermochim. Acta* **2016**, *638*, 35–43.

(33) Kong, W.; Lei, Y.; Jiang, Y.; Lei, J. Preparation and thermal performance of polyurethane/PEG as novel form-stable phase change materials for thermal energy storage. *J. Therm. Anal. Calorim.* **2017**, *130*, 1011–1019.

(34) Chen, Y.; Zhao, L.; Shi, Y. Preparation of polyvinyl chloride capsules for encapsulation of paraffin by coating multiple organic/inorganic layers. *J. Taiwan Inst. Chem. Eng.* **2017**, *77*, 177–186.

(35) Wu, H.-y.; Li, S.-t.; Shao, Y.-w.; Jin, X.-z.; Qi, X.-d.; Yang, J.-h.; Zhou, Z.-w.; Wang, Y. Melamine foam/reduced graphene oxide supported form-stable phase change materials with simultaneous shape memory property and light-to-thermal energy storage capability. *Chem. Eng. J.* **2020**, *379*, 122373.

(36) Zhang, Q.; Cui, K.; Feng, J.; Fan, J.; Li, L.; Wu, L.; Huang, Q. Investigation on the recovery performance of olefin block copolymer/hexadecane form stable phase change materials with shape memory properties. *Sol. Energy Mater. Sol. Cells* **2015**, *132*, 632–639.

(37) Wu, W.; Wu, W.; Wang, S. Form-stable and thermally induced flexible composite phase change material for thermal energy storage and thermal management applications. *Appl. Energy* **2019**, *236*, 10–21.

(38) Zhang, Q.; Feng, J. Difunctional olefin block copolymer/paraffin form-stable phase change materials with simultaneous shape memory property. *Sol. Energy Mater. Sol. Cells* **2013**, *117*, 259–266.

(39) Wang, Y.; Zhang, Z.; Zhang, T.; Qin, Z.; Zhang, D.; Ji, H. Preparation and characterization of erythritol/Graphene Oxide Shape-Stable composites with improved thermal-physical property. *ChemistrySelect* **2019**, *4*, 1149–1157.

(40) Sun, K.; Kou, Y.; Zheng, H.; Liu, X.; Tan, Z.; Shi, Q. Using silicagel industrial wastes to synthesize polyethylene glycol/silica-hydroxyl form-stable phase change materials for thermal energy storage applications. *Sol. Energy Mater. Sol. Cells* **2018**, *178*, 139–145.

(41) Yazdani, M. R.; Etula, J.; Zimmerman, J. B.; Seppälä, A. Ionic cross-linked polyvinyl alcohol tune vitrification and coldcrystallization of sugar alcohol for long-term thermal energy storage. *Green Chem.* **2020**, *22*, 5447.